^{2}H Quadrupolar Coupling Constant: A Spectroscopic Ruler for Transition Metal–Hydride Bond Distances in Molecular and Surface Sites

Domenico Gioffrè, [a] Cäcilie Müller, [a,] Scott R. Docherty, [a,†] Alexander Yakimov, [a] Christophe Copéret[a,*]

[a]*Department of Chemistry and Applied Biosciences, ETH Zürich, CH-8093 Zürich, Switzerland*

[†]*Department of Chemistry, Columbia University, New York, NY 10027, United States*

ABSTRACT: Transition-metal hydrides (TMHs) find numerous applications across fields, from catalysis to H_2 storage. Yet, determining the structure of TMHs can remain a challenge, as hydrogen is difficult to detect by X-ray based or classical spectroscopic techniques. Considering that deuterium isotope (D) is a quadrupolar nucleus (I = 1) and that a quadrupolar coupling constant (C_Q) depends on the distance between D and its bonding partner E (d_{ED}), we evaluate this trend across molecularly-defined transition-metal deuterides (TMDs) through a systematic investigation across TM block elements using both computations and experiments. We show that the M–D bond distance (d_{MD}) in [Å] correlates with the C_Q values in [kHz] as $d_{MD} = 7.83(C_Q + 28.7)^{-1/3}$ - independently from the nature of the TM - with an accuracy > 0.04-0.08 Å. Based on experimental C_Q values measured by ^{2}H solid-state NMR, this simple correlation is then used to obtain the M-D bond distances in two silica-supported TMDs (M = Zr and Ir), notable heterogeneous catalysts, representing early and late TMDs, where evaluating M-D bond distances by other means is very challenging. Considering the ease of measurement, this method is readily applicable to a large range of diamagnetic terminal M–Ds, from molecular to surface sites, making ^{2}H NMR a method of choice to measure TMDs bond distances.

Transition-metal hydrides (TMHs)[1–3] are used in numerous applications, from stoichiometric reagents to reduce functional groups in organic synthesis (e.g. carbonyl or carboxyl groups) to key reaction intermediates in catalytic reactions such as hydrogenation and de-hydrogenation, to name but a few.[4–10] They are also involved in the functionalization of C-H bonds and are known to promote alkane hydrogenolysis and metathesis, reactions that have recently found applications in polyolefin upcycling (Fig. 1a).[11–24] TMHs are also key intermediates in CO_x conversion technologies and central to H_2/energy storage and sensing technologies.[25,26] Despite the broad interest and years of research on TMHs, their characterization remains challenging (Fig. 1b). For instance, infrared (IR) spectroscopy can, in principle, provide structural insights on the nature of M-H bonds,[27] but IR bands are often weak due to their low dipole moment and/or appear in regions overlapping with other functional groups or supporting material features.[4,11] Regarding X-ray based techniques, they are usually not suitable to locate proton atoms of M-H species, therefore deuterium labelling is needed to determine M-D distances in molecules through single crystal neutron diffraction. However, this technique relies on the existence of long-range structural order making them not suitable for all materials. Inelastic neutron scattering (INS) techniques overcome this limitation, but are often challenging due to the need for large amounts of sample and the access to spallation source.[28–33] In addition, while ^{1}H NMR spectroscopy is a powerful tool to identify MHs due to their observation in a particularly large chemical shift window (> 40 ppm), their NMR chemical shift (δ_{iso}) can be difficult to rationalize because it is dominated by the 'spin-orbit heavy-atom effect on the light-atom' (SO-HALA effect).[34] Furthermore, while $J_{H\text{-}H}/J_{H\text{-}D}$ ^{1}H NMR measurements of metal polyhydrides have been applied to understand the bonding order with H atoms, differentiating between H_2 and metal-hydride

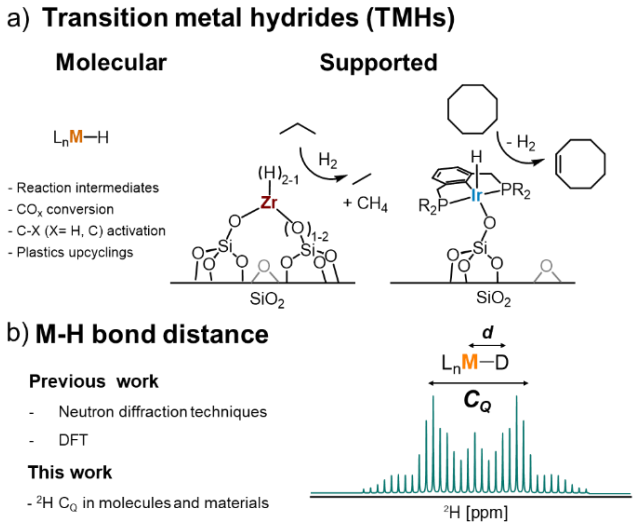

Figure 1. a) Representative reactivities of TMHs and supported TMHs studied in this work; b) Spectroscopic tools for the M-H(D) bond distance determination.

https://doi.org/10.26434/chemrxiv-2025-6mvmv **ORCID:** https://orcid.org/0000-0003-2208-4148

complexes, they do not provide direct insights into the M–H bonding situation.[3,10,35–37] In that respect, ^{2}H solid-state (ss) NMR can be particularly powerful to characterize the corresponding metal deuterides (MD) as found in molecular, surface or bulk species.[38–40] Indeed, ^{2}H ss-NMR provides access to the same δ_{iso} as ^{1}H, and is characterized by two additional parameters characteristic of the local environment due to its integer nuclear spin (I = 1): the quadrupolar coupling constant (C_Q) and the asymmetry parameter (η). For instance, η is directly related to the binding mode of D to metal sites: while terminal MDs display a characteristic η = 0, bridging MDs have η > 0.1.[38,39] Furthermore, the magnitude of C_Q has been shown to qualitatively relate to the bond distance between D and the atom directly bound to it, in both organic and inorganic molecular systems and bulk materials, with shorter bond lengths leading to higher C_Q values.[40–43] Both observations can be traced back to simple electrostatic interactions of the quadrupole moment of D with its electric field gradient (EFG) tensor.[38] The relation between C_Q and element-deuterium distance (E–D) in a molecule can be derived from the equation of the EFG along its principal component (q_{zz}, eq.1-2), aligned to the E-D bond, to which C_Q is proportional (eq.1). Namely, assigning the deuteron to the origin of molecular coordinates, q_{zz} can be obtained as a sum over the nuclear (n) and electron (i) contributions, having r_n and r_i distances from D. In the case of linear MDs, the nuclear term can be approximated so that it only accounts for the M atom directly bound to D (eq.3; details in ESI).[44–50]

$$C_Q = \frac{eQV_{zz}}{h} = \frac{e^2Qq_{zz}}{h} \quad (1)$$

$$q_{zz} = \sum_n Z_n \frac{(3cos^2\theta-1)}{r_n^3} - e\left\langle \Psi^* \middle| \sum_i \frac{(3cos^2\theta-1)}{r_i^3} \middle| \Psi \right\rangle \quad (2)$$

$$q_{zz} \cong \frac{2Z_M}{d_{MD}^3} - e\left\langle \Psi^* \middle| \sum_i \frac{(3cos^2\theta-1)}{r_i^3} \middle| \Psi \right\rangle \quad (3)$$

Empirical correlations between C_Q and bond distances in organic species has confirmed the scaling factor of d_{ED}^{-3}, and experimental observation on metal deuterides in Zintl phases and in bulk materials show a similar trend.[40,48,49] Considering the importance of TMDs in catalysis, we evaluate here the correlation between the C_Q and M–D bond distance in a series of molecularly-defined TMDs, using a combined experimental and computational approach. This study shows that such correlation is independent from the nature of the transition metal, TM. A systematic study of the calculated ^{2}H NMR fingerprints of TMD across the periodic table using DFT computations benchmarked by experimental ^{2}H NMR data allowed us to derive an empirical correlation between the M–D bond length (d_{MD}/Å) and C_Q (kHz) values. Notably, C_Q is independent of the nature of M, making this correlation general across terminal TMDs. This study provides a robust methodology to evaluate the M-H(D) distance from simple ^{2}H NMR methods. The large chemical space explored provides expected ranges of C_Q and M-D distances across the TM block series and can be used to estimate bond distances in molecular species for which single crystal to neutron diffraction techniques cannot be applied. The generality of this approach also enables to deduct bond distances in supported MDs, here exemplified with prototypical early and late TM systems prepared *via* Surface Organometallic Chemistry (SOMC) techniques, namely the silica-supported Zr-(H/D)$_x$/SiO$_2$ used for plastics and hydrocarbon conversion, and a supported Ir-(H/D) pincer complex, (PCP)Ir-(H/D)/SiO$_2$ [PCP = 2,6-C$_6$H$_3$(CH$_2$P^{t}Bu$_2$)$_2$], active toward (de)hydrogenation of liquid and gaseous hydrocarbons.[51,52] Because of the scarcity of experimental C_Q values and available INS data on molecularly-defined TMDs, we first carried out DFT calculations across a series of known diamagnetic molecular terminal TMDs to evaluate their ^{2}H NMR parameters (adf2022, ZORA, hybrid PBE0/TZ2P).[39] We included complexes from group 4 to 10 and from the 3rd to 5th row, with both neutral and charged compounds and a range of ligands (computational details, the list of species and the computed and experimental parameters are reported in the SI). Note that, at this level of theory, the computed ^{1}H chemical shift values (δ_{iso}) of these metal hydrides agree well with literature values (Fig. S14, R^2=0.98), indicating that the electronic structures are well-described. Similarly, the calculated C_Q values and M-D distances compare well with experimental data from C_Q determined with either T_1 relaxation measurement or ^{2}H solid-state NMR at low temperature[39] (Fig. S15a, R^2=0.93) and M-D distances from single-crystal INS (Fig. S15b, R^2=0.81)].

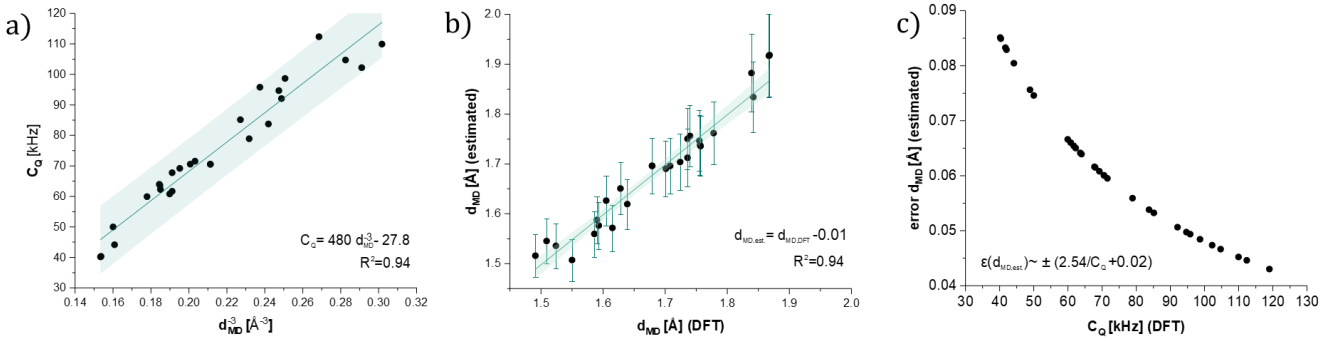

Figure 2. Computed C_Q values (kHz) of a series of TMDs vs. a) their computed d_{MD}^{-3}. b) Comparison between the d_{MD} values (estimated from C_Q) and the computed values. c) Error of the estimated d_{MD} as function of C_Q. The linear fittings (blue trend lines) and the corresponding R^2 value are reported. The blue shaded area represents 95% confidence interval.

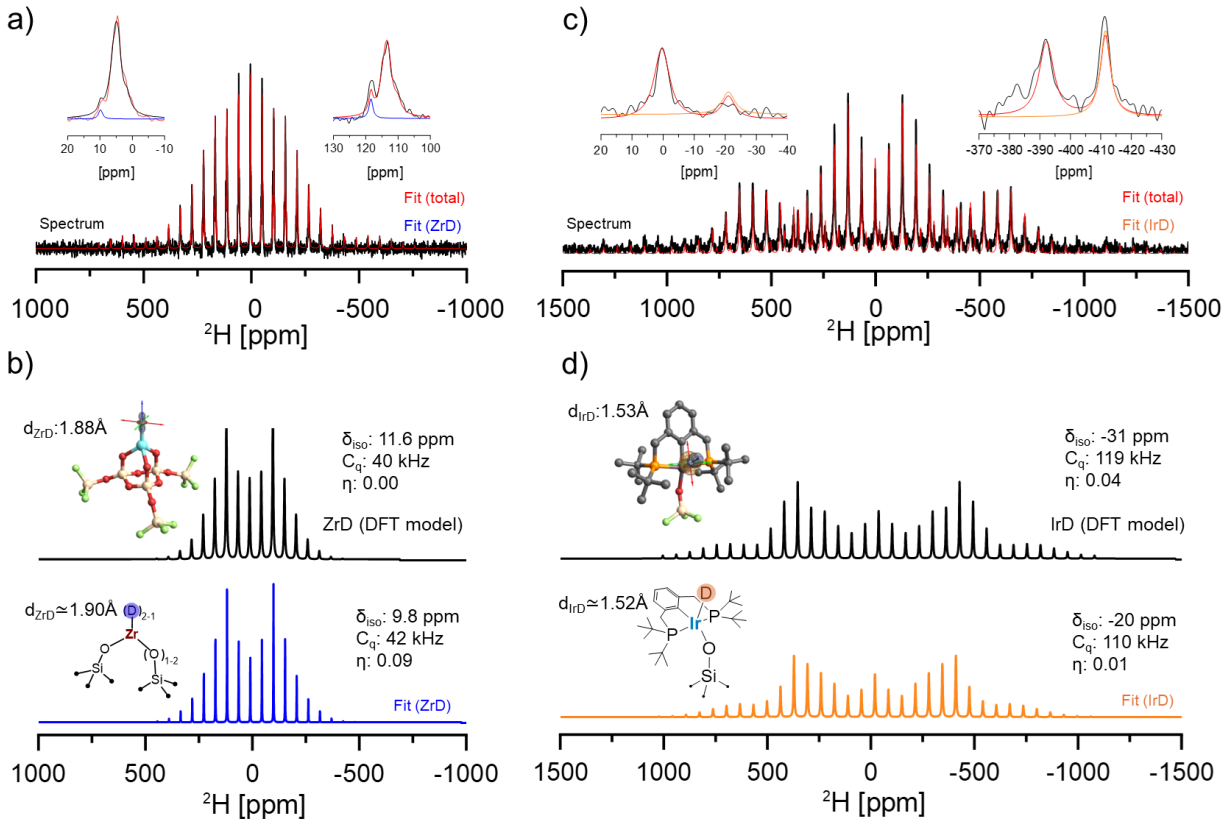

Figure 3. ^{2}H ss-NMR, numerical fittings and DFT models of a-b) ZrD_x/SiO_2 (14.1 T, 111 K, MAS: 5 kHz); reproduced from our previous work;[39] and c-d) (PCP)IrD/SiO_2 (14.1 T, 111 K, MAS: 6 kHz). Fitting deconvolution at the central sideband and at the sideband with highest intensity for the MD species are shown (inset, details in ESI). Visualization of EFG tensors for the DFT F-terminated SiO_2 cluster models; the orientation of V_{ZZ} represented by blue axis, V_{YY} by red, and V_{XX} by green.

Overall, the robustness of the calculations was verified for the following ranges: 7.6 > δ_{iso}(ppm) > -31.2, 87 > C_Q(kHz) > 47 and M-D bond lengths in the range of 1.77 > d_{MD}(Å) > 1.54. Having established a computational protocol to reliably calculate the structure and ^{2}H NMR fingerprints of TMDs across the periodic table, we next evaluate potential relationship between computed C_Q and d_{MD}. The C_Q values decrease as the M-D bond lengthens, as previously discussed for other elements, and in agreement with the mathematical formulation of C_Q ($\propto d_{MD}^{-3}$, R^2=0.97) (Fig. 2a, Fig. S16). The longer distances and smaller C_Q values are found for early TMDs (*e. g.* 1.87 Å for $Cp^*_2ZrD_2$), while the shortest ones and larger C_Q values are observed for late TMDs (*e. g.* 1.55 Å for (PCP)IrD(OPh). Notably, independently of the identity of M, C_Q correlates linearly with d_{MD}^{-3} (Fig. 2a), according to the empirical expression in eq. 4. Therefore, measuring C_Q (kHz) enables to ascertain the M–D bond distances (Å) in terminal hydrides according to eq. 5 (Fig. 2b, details in ESI), with an accuracy between 0.08 and 0.04 Å (Fig. 2c, details in ESI).

$$C_Q \cong \frac{480 \pm 24}{d_{MD}{}^3} - (27.8 \pm 5.2) \quad (4)$$

$$d_{MD} \cong \frac{7.83}{(C_Q+27.8)^{1/3}} \pm \frac{2.54}{(C_Q+0.02)^{1/3}} \quad (5)$$

We find worth mentioning that obtaining ^{2}H C_Q from ss-NMR methods is more robust than using T_1 relaxation experiments in solution, because of possible H/D-exchange reactions, that can yield misleading conclusions regarding d_{MD} estimation (see ESI for discussion). Having established that the ^{2}H C_Q encodes information regarding the bond distance of molecular MDs, we next used this approach to measure the M-D bond distances in supported TMDs, which are not readily available *via* (conventional) characterisation techniques. We selected two silica-supported (early and late) TMDs, prepared *via* SOMC techniques, namely i) the silica-supported zirconium hydrides, known for their catalytic properties in hydrocarbon conversion processes including polyolefin upcycling,[16,21] and ii) the silica-supported iridium hydrides, stabilized by pincer PCP phosphine ligand (PCP)Ir-(H/D), known to catalyze hydrocarbon (de)hydrogenation reactions at low temperatures.[51,52] We first measured their ^{2}H ss-NMR spectra and extracted the quadrupolar NMR parameters, C_Q and h, for each deuterium species through deconvolution and fitting of the NMR lineshapes (experimental and fitting details are found in ESI). For the supported Zr-system, fitting the NMR lineshape of the ^{2}H NMR of the deuteride prepared by H/D exchange reaction (see ESI for details) show the presence of several deuterium species (Fig. 3a): $Zr(D)_x$ species associated with $\delta_{iso}/C_Q/\eta$ values of 9.8 ppm / 42 kHz / 0.09 (Fig.3a-b, blue line) along with Si-D_x (with $\delta_{iso}/C_Q/\eta$ values of 5.2 ppm / 42 kHz / 0.60 and 4.34 ppm / 58 kHz / 0.97) and C-D (1.5 ppm / 96 kHz / 0.99) from remaining organic moieties of the OM Zr precursor.[39] Notably, the measured δ_{iso}/C_Q parameters of the silica-

supported ZrH(D) are similar to these of $Cp^*_2ZrD_2$ molecular compounds (7.46 ppm/40 kHz), in agreement with their chemical similarity. Using the developed empirical correlation (*vide supra*) to the experimental C_Q of the supported ZrD_x/SiO_2 (42 kHz, Fig. 3a-b, blue line) provides an estimated d_{ZrD} distance of 1.90 ± 0.08 Å. This value lies in the same range of distances computed for $Cp^*_2ZrD_2$ (1.87 Å) and the value obtained for the DFT model, based on a F-terminated SiO_2 cluster (1.88 Å, Fig. 3b, black line).[39]

We next measured the ^{2}H NMR parameters of (PCP)IrD(H/D)/SiO_2 surface species,[51,52] prepared by grafting (PCP)IrD_4 on deuterated SiO_2 (see ESI for further details and routine characterization). The ^{2}H ss-NMR spectrum of (PCP)IrD/SiO_2 (Fig. 3c, 110 K, MAS 6 kHz) reveals the presence of four different deuterium species from numerical fittings (Fig. 3b, Fig. S12). The signal associated with $\delta_{iso}/C_Q/\eta$ = –20 ppm / 110 kHz / 0.0 (Fig. 3c, orange line) was assigned to a linear Ir-D, as it shows comparable NMR fingerprints to the isostructural (PCP)IrH(OPh) molecular complex (–32 ppm, 112 kHz) and a F-terminated DFT model (–31 ppm, 119 kHz, Fig. 3d, black line, Fig. S13). The estimation of d_{IrD} for the supported (PCP)IrD/SiO_2 system from the measured C_Q value of 110 kHz is evaluated as 1.52 ± 0.04 Å, in the range of the molecular (PCP)IrD(OPh) (1.55 Å) and the DFT model (1.53 Å). Additional species were found to have $\delta_{iso}/C_Q/\eta$ values of 1.1 ppm / 102 kHz / 0.6 and 2.5 ppm / 179 kHz / 0.0, assigned to the C-D bonds of the CH_2 and ^{t}Bu groups of the PCP ligand, as already found for the deuterated molecular precursor (Fig. S8). Additionally, a deuterium species with $\delta_{iso}/C_Q/\eta$ values of 1.8 ppm / 60 kHz / 0.0, was assigned to Si-OD, which have been previously reported to be in this range (Fig. S12).[53]

Overall, this work demonstrates how ^{2}H ss-NMR parameters provide a molecular-level understanding of the structure of supported TMH(D). Specifically, readily measurable quadrupolar coupling constant (C_Q) of terminal TMDs can be used as a spectroscopic ruler to deduct the M–D bond distance through the empirical correlation (eq. 5) with a good precision (0.04-0.08Å). This methodology is applicable to both molecular and supported systems, including materials with low M loadings, where neutron diffraction studies suffer from their intrinsic low sensitivity. The robustness of this approach is illustrated by its applications to a broad range of molecules and materials, establishing ^{2}H ss-NMR as a readily available tool to measure M–H bond distances in transition-metal hydrides *via* simple H/D exchange reaction and measurement of ^{2}H NMR parameters.

AUTHOR INFORMATION

Corresponding Author

Christophe Copéret – Department of Chemistry and Applied Biosciences, ETH Zürich, CH-8093 Zürich, Switzerland; orcid.org/0000-0001-9660-3890; Email: ccoperet@ethz.ch

Authors

Domenico Gioffrè – Department of Chemistry and Applied Biosciences, ETH Zürich, CH-8093 Zürich, Switzerland; orcid.org/0000-0003-2208-4148;

Cäcilie Müller – Department of Chemistry and Applied Biosciences, ETH Zürich, CH-8093 Zürich, Switzerland; orcid.org/0009-0001-3049-9928;

Scott R. Docherty – Department of Chemistry and Applied Biosciences, ETH Zürich, CH-8093 Zürich, Switzerland; orcid.org/0000-0002-8605-3669

Alexander Yakimov – Department of Chemistry and Applied Biosciences, ETH Zürich, CH-8093 Zürich, Switzerland; orcid.org/0000-0002-8624-1002;

Present Address

†**Scott R. Docherty** – Department of Chemistry, Columbia University, New York, NY 10027, United States

Funding Sources

Swiss National Science Foundation is acknowledged for founding: grants 200020B_192050 and 200021L_213070 (D.G, C.C.); grants 200021_169134, and 200020B_192050 (S.R.D, C. C.). C.C. and A. Y. gratefully acknowledge ETH+ Project SynthMatLab for financial support. DFT computations were run on the Euler Cluster (ETH Zürich).

ACKNOWLEDGMENT

Dr. Shahar Dery (ETH Zürich) is thankfully acknowledged for providing the deuterated SiO_2 support. Philip Schärz (ETH Zürich) is acknowledged for preliminary studies on the (PCP)IrD_4 system.

ABBREVIATIONS

ss-NMR, solid-state nuclear magnetic resonance; C_Q, quadrupolar coupling constant, IR, Infrared, INS, inelastic neutron scattering, DFT, Density Functional Theory; EFG, electric field gradient; SO-HALA, spin-orbit heavy-atom effect on the light-atom; TMH(D), transition metal hydride (deuteride).

REFERENCES

(1) Crabtree, R. H. Hydride Complexes of the Transition Metals. In *Encyclopedia of Inorganic and Bioinorganic Chemistry*; John Wiley & Sons, Ltd, 2011.

(2) Morris, R. H. Hydride Complexes of the Transition Metals. In *Encyclopedia of Inorganic and Bioinorganic Chemistry*; John Wiley & Sons, Ltd, 2018; pp 1–12.

(3) Kubas, G. J. Dihydrogen Complexes as Prototypes for the Coordination Chemistry of Saturated Molecules. *Proc. Natl. Acad. Sci.* **2007**, *104* (17), 6901–6907.

(4) Jordan, A. J.; Lalic, G.; Sadighi, J. P. Coinage Metal Hydrides: Synthesis, Characterization, and Reactivity. *Chem. Rev.* **2016**, *116* (15), 8318–8372.

(5) Esteruelas, M. A.; López, A. M.; Oliván, M. Polyhydrides of Platinum Group Metals: Nonclassical Interactions and σ-Bond Activation Reactions. *Chem. Rev.* **2016**, *116* (15), 8770–8847.

(6) Crossley, S. W. M.; Obradors, C.; Martinez, R. M.; Shenvi, R. A. Mn-, Fe-, and Co-Catalyzed Radical Hydrofunctionalizations of Olefins. *Chem. Rev.* **2016**, *116* (15), 8912–9000.

(7) Kaphan, D. M.; Ferrandon, M. S.; Langeslay, R. R.; Celik, G.; Wegener, E. C.; Liu, C.; Niklas, J.; Poluektov, O. G.; Delferro, M. Mechanistic Aspects of a Surface Organovanadium(III) Catalyst for Hydrocarbon Hydrogenation and Dehydrogenation. *ACS Catal.* **2019**, *9* (12), 11055–11066.

(8) Sabo-Etienne, S.; Chaudret, B. Chemistry of Bis(Dihydrogen) Ruthenium Complexes and of Their Derivatives. *Coord. Chem. Rev.* **1998**, *178–180*, 381–407.

(9) Clapham, S. E.; Iuliis, M. Z.-D.; Mack, K.; Prokopchuk, D. E.; Morris, R. H. Alcohol-Assisted Base-Free Hydrogenation of Acetophenone Catalyzed by $OsH(NHCMe_2CMe_2NH_2)(PPh_3)_2$. *Can. J. Chem.* **2014**, *92* (8), 731–738.

(10) Maltby, P. A.; Schlaf, M.; Steinbeck, M.; Lough, A. J.; Morris, R. H.; Klooster, W. T.; Koetzle, T. F.; Srivastava, R. C. Dihydrogen with Frequency of Motion Near the 1H Larmor Frequency. Solid-State Structures and Solution NMR Spectroscopy of Osmium Complexes Trans-$[Os(H{\cdot\cdot}H)X(PPh_2CH_2CH_2PPh_2)_2]$+ (X = Cl, Br). *J. Am. Chem. Soc.* **1996**, *118* (23), 5396–5407.

(11) Copéret, C.; Estes, D. P.; Larmier, K.; Searles, K. Isolated Surface Hydrides: Formation, Structure, and Reactivity. *Chem. Rev.* **2016**, *116* (15), 8463–8505.

(12) Wang, J.; Li, G.; Li, Z.; Tang, C.; Feng, Z.; An, H.; Liu, H.; Liu, T.; Li, C. A Highly Selective and Stable ZnO-ZrO2 Solid Solution Catalyst for CO2 Hydrogenation to Methanol. *Sci. Adv.* **2017**, *3* (10), e1701290.

(13) Zhao, D.; Tian, X.; Doronkin, D. E.; Han, S.; Kondratenko, V. A.; Grunwaldt, J.-D.; Perechodjuk, A.; Vuong, T. H.; Rabeah, J.; Eckelt, R.; Rodemerck, U.; Linke, D.; Jiang, G.; Jiao, H.; Kondratenko, E. V. In Situ Formation of ZnOx Species for Efficient Propane Dehydrogenation. *Nature* **2021**, *599* (7884), 234–238.

(14) Castro-Fernández, P.; Mance, D.; Liu, C.; Moroz, I. B.; Abdala, P. M.; Pidko, E. A.; Copéret, C.; Fedorov, A.; Müller, C. R. Propane Dehydrogenation on Ga2O3-Based Catalysts: Contrasting Performance with Coordination Environment and Acidity of Surface Sites. *ACS Catal.* **2021**, *11* (2), 907–924.

(15) Edenfield, W. C.; Mason, A. H.; Lai, Q.; Agarwal, A.; Kobayashi, T.; Kratish, Y.; Marks, T. J. Rapid Polyolefin Plastic Hydrogenolysis Mediated by Single-Site Heterogeneous Electrophilic/Cationic Organo-Group IV Catalysts. *ACS Catal.* **2024**, *14* (1), 554–565.

(16) Dufaud, V.; Basset, J.-M. Catalytic Hydrogenolysis at Low Temperature and Pressure of Polyethylene and Polypropylene to Diesels or Lower Alkanes by a Zirconium Hydride Supported on Silica-Alumina: A Step Toward Polyolefin Degradation by the Microscopic Reverse of Ziegler–Natta Polymerization. *Angew. Chem. Int. Ed.* **1998**, *37* (6), 806–810.

(17) Chen, H.; Gao, P.; Liu, Z.; Liang, L.; Han, Q.; Wang, Z.; Chen, K.; Zhao, Z.; Guo, M.; Liu, X.; Han, X.; Bao, X.; Hou, G. Direct Detection of Reactive Gallium-Hydride Species on the Ga2O3 Surface via Solid-State NMR Spectroscopy. *J. Am. Chem. Soc.* **2022**, *144* (38), 17365–17375.

(18) Yermakovt, Y. I.; Ryndin, Y. A.; Alekseev, O. S.; Kochubey, D. I.; Shmachkov, V. A.; Gergert, N. I. Hydride Complexes of Titanium and Zirconium Attached to SiO2 as Hydrogenation Catalysts. *J. Mol. Catal.* **1989**, *49* (2), 121–132.

(19) Basset, J.-M.; Coperet, C.; Soulivong, D.; Taoufik, M.; Cazat, J. T. Metathesis of Alkanes and Related Reactions. *Acc. Chem. Res.* **2010**, *43* (2), 323–334.

(20) Coperet, C. C−H Bond Activation and Organometallic Intermediates on Isolated Metal Centers on Oxide Surfaces. *Chem. Rev.* **2010**, *110* (2), 656–680.

(21) Celik, G.; Kennedy, R. M.; Hackler, R. A.; Ferrandon, M.; Tennakoon, A.; Patnaik, S.; LaPointe, A. M.; Ammal, S. C.; Heyden, A.; Perras, F. A.; Pruski, M.; Scott, S. L.; Poeppelmeier, K. R.; Sadow, A. D.; Delferro, M. Upcycling Single-Use Polyethylene into High-Quality Liquid Products. *ACS Cent. Sci.* **2019**, *5* (11), 1795–1803.

(22) Lai, Q.; Mason, A. H.; Agarwal, A.; Edenfield, W. C.; Zhang, X.; Kobayashi, T.; Kratish, Y.; Marks, T. J. Rapid Polyolefin Hydrogenolysis by a Single-Site Organo-Tantalum Catalyst on a Super-Acidic Support: Structure and Mechanism. *Angew. Chem.* **2023**, *135* (50), e202312546.

(23) Kanbur, U.; Zang, G.; Paterson, A. L.; Chatterjee, P.; Hackler, R. A.; Delferro, M.; Slowing, I. I.; Perras, F. A.; Sun, P.; Sadow, A. D. Catalytic Carbon-Carbon Bond Cleavage and Carbon-Element Bond Formation Give New Life for Polyolefins as Biodegradable Surfactants. *Chem* **2021**, *7* (5), 1347–1362.
(24) Pichugov, A. V.; Escomel, L.; Lassalle, S.; Petit, J.; Jabbour, R.; Gajan, D.; Veyre, L.; Fonda, E.; Lesage, A.; Thieuleux, C.; Camp, C. Highly Selective and Efficient Perdeuteration of N-Pentane via H/D Exchange Catalyzed by a Silica-Supported Hafnium-Iridium Bimetallic Complex. *Angew. Chem. Int. Ed.* **2024**, *63* (16), e202400992.
(25) Bhuiya, M. M. H.; Kumar, A.; Kim, K. J. Metal Hydrides in Engineering Systems, Processes, and Devices: A Review of Non-Storage Applications. *Int. J. Hydrog. Energy* **2015**, *40* (5), 2231–2247.
(26) Kaeffer, N.; Leitner, W. Electrocatalysis with Molecular Transition-Metal Complexes for Reductive Organic Synthesis. *JACS Au* **2022**, *2* (6), 1266–1289.
(27) Morris, R. H. Relationship between Transition-Metal Hydride Bond Lengths and Stretching Wavenumbers. *Inorg. Chem.* **2024**.
(28) Polo-Garzon, F.; Luo, S.; Cheng, Y.; Page, K. L.; Ramirez-Cuesta, A. J.; Britt, P. F.; Wu, Z. Neutron Scattering Investigations of Hydride Species in Heterogeneous Catalysis. *ChemSusChem* **2019**, *12* (1), 93–103.
(29) Woińska, M.; Grabowsky, S.; Dominiak, P. M.; Woźniak, K.; Jayatilaka, D. Hydrogen Atoms Can Be Located Accurately and Precisely by X-Ray Crystallography. *Sci. Adv.* **2016**, *2* (5), e1600192.
(30) Murphy, V. J.; Rabinovich, D.; Hascall, T.; Klooster, W. T.; Koetzle, T. F.; Parkin, G. False Minima in X-Ray Structure Solutions Associated with a "Partial Polar Ambiguity": Single Crystal X-Ray and Neutron Diffraction Studies on the Eight-Coordinate Tungsten Hydride Complexes, $W(PMe_3)_4H_2X_2$ (X = F, Cl, Br, I) and $W(PMe_3)_4H_2F(FHF)$. *J. Am. Chem. Soc.* **1998**, *120* (18), 4372–4387.
(31) Bennett, E. L.; Murphy, P. J.; Imberti, S.; Parker, S. F. Characterization of the Hydrides in Stryker's Reagent: $[HCu\{P(C_6H_5)_3\}]_6$. *Inorg. Chem.* **2014**, *53* (6), 2963–2967.
(32) Yvon, K.; Kohlmann, H.; Bertheville, B. Europium–Hydrogen Bond Distances in Saline Metal Hydrides by Neutron Diffraction. *CHIMIA* **2001**, *55* (6), 505–505.
(33) Albinati, A.; Grellier, M.; Ollivier, J.; Georgiev, P. A. On the Energetics of Binding and Hydride Exchange in the $RuH_2(H_2)_2[P(C_5H_9)_3)]_2$ Complex as Revealed by Inelastic Neutron Scattering and DFT Studies. *New J. Chem.* **2022**, *46* (30), 14649–14659.
(34) Vícha, J.; Novotný, J.; Komorovsky, S.; Straka, M.; Kaupp, M.; Marek, R. Relativistic Heavy-Neighbor-Atom Effects on NMR Shifts: Concepts and Trends Across the Periodic Table. *Chem. Rev.* **2020**, *120* (15), 7065–7103.
(35) Hebden, T. J.; Goldberg, K. I.; Heinekey, M. D.; Zhang, X.; Emge, T. J.; Goldman, A. S.; Krogh-Jespersen, K. Dihydrogen/Dihydride or Tetrahydride? An Experimental and Computational Investigation of Pincer Iridium Polyhydrides. *Inorg. Chem.* **2010**, *49* (4), 1733–1742.
(36) Luther, T. A.; Heinekey, D. M. Synthesis, Characterization, and Reactivity of Dicationic Dihydrogen Complexes of Osmium and Ruthenium. *Inorg. Chem.* **1998**, *37* (1), 127–132.
(37) Sabo-Etienne, S.; Chaudret, B. Quantum Mechanical Exchange Coupling in Polyhydride and Dihydrogen Complexes. *Chem. Rev.* **1998**, *98* (6), 2077–2092.
(38) Butler, L. G.; Keiter, E. A. Interpretation of Electric Field Gradients at Deuterium as Measured by Solid-State Nmr Spectroscopy. *J. Coord. Chem.* **1994**, *32* (1–3), 121–134.
(39) Docherty, S. R.; Schärz, P.; Gioffrè, D.; Yakimov, A. V.; Copéret, C. Probing the Nature of Surface Hydrides by Deuterium Quadrupolar Parameters: A Case Study on Silica-Supported Zirconium Hydrides. *Helv. Chim. Acta* **2023**, *107 (1)*, e202300173.
(40) Guehne, R.; Auer, H.; Kohlmann, H.; Haase, J.; Bertmer, M. Determination of Element–Deuterium Bond Lengths in Zintl Phase Deuterides by ^{2}H-NMR. *Phys. Chem. Chem. Phys.* **2019**, *21* (20), 10594–10602.
(41) Nietlispach, D.; Bakhmutov, V. I.; Berke, H. Deuterium Quadrupole Coupling Constants and Ionic Bond Character in Transition Metal Hydride Complexes from 2H NMR T1 Relaxation Data in Solution. *J. Am. Chem. Soc.* **1993**, *115* (20), 9191–9195.
(42) Gilson, D. F. R.; Morin, F. G.; Moyer, R. O. Deuterium NMR and Differential Scanning Calorimetric Studies of the Calcium Salts of Rhodium and Iridium Pentadeuterides, Ca_2RhD_5 and Ca_2IrD_5. *J. Phys. Chem. B* **2006**, *110* (33), 16487–16490.
(43) Moyer, R. O.; Antao, S. M.; Toby, B. H.; Morin, F. G.; Gilson, D. F. R. Neutron Powder Diffraction and Solid-State Deuterium NMR Studies of Ca_2RuD_6 and the Stability of Transition Metal Hexahydride Salts. *J. Alloys Compd.* **2008**, *460* (1), 138–141.
(44) Badger, R. M. A Relation Between Internuclear Distances and Bond Force Constants. *Relat. Internuclear Distances Bond Force Constants* **1934**, *2*.
(45) Foley, H. M.; Sternheimer, R. M.; Tycko, D. Nuclear Quadrupole Coupling in Polar Molecules. *Phys. Rev.* **1954**, *93* (4), 734–742.
(46) Bersohn, R. Electric Field Gradients in Ionic Crystals. I. Nuclear Quadrupole Coupling Constants. *J. Chem. Phys.* **2004**, *29* (2), 326–333.

(47) Guo, K. Interpretation of Solid State Deuterium NMR Spectroscopic Parameters. Doctor of Philosophy, Louisiana State University and Agricultural & Mechanical College, 1989.
(48) Huber, H. Deuterium Quadrupole Coupling Constants. A Theoretical Investigation. *J. Chem. Phys.* **1985**, *83* (9), 4591–4598.
(49) Huber, H. The Electric Field Gradient at Hydrogen and Its First and Second Derivatives with Respect to the X-H Bond-Length for First- and Second-Row Hydrides. *J. Mol. Struct. THEOCHEM* **1985**, *121*, 207–211.
(50) Salem, L. Theoretical Interpretation of Force Constants. *Theor. Interpret. Force Constants* **1963**, *38*, 1227.
(51) Rimoldi, M.; Mezzetti, A. Batch and Continuous Flow Hydrogenation of Liquid and Gaseous Alkenes Catalyzed by a Silica-Grafted Iridium(III) Hydride. *Helv. Chim. Acta* **2016**, *99* (12), 908–915.
(52) Rimoldi, M.; Mezzetti, A. Silica-Grafted 16-Electron Hydride Pincer Complexes of Iridium(III) and Their Soluble Analogues: Synthesis and Reactivity with CO. *Inorg. Chem.* **2014**, *53* (22), 11974–11984.
(53) Kobe, J. M.; Gluszak, T. J.; Dumesic, J. A.; Root, T. W. Deuterium NMR Characterization of Broested Acid Sites and Silanol Species in Zeolites. *J. Phys. Chem.* **1995**, *99* (15), 5485–5491.

Table of Contents: